RESEARCH ARTICLE

Macromolecular Materials and Engineering

www.mame-journal.de

How Nanofibers Carry the Load: Toward a Universal and Reliable Approach for Tensile Testing of Polymeric Nanofibrous Membranes

Emanuele Maccaferri, Davide Cocchi, Laura Mazzocchetti, Tiziana Benelli, Tommaso Maria Brugo, Loris Giorgini, and Andrea Zucchelli**

Nanofibrous nonwovens show high versatility and outstanding properties, with reduced weight. Porous morphology, high material flexibility and deformability challenge their mechanical testing, severely affecting results reliability. Still today, a specific technical standard method to carry out tensile testing of nonwoven nanofibrous mats is lacking, as well as studies concerning tensile test data reliability. In this work, an accurate, systematic, and critical study is presented concerning tensile testing of nonwovens, using electrospun Nylon 66 random nanofibrous mats as a case study. Nanofibers diameter and specimen geometry are investigated to thoroughly describe the nanomat tensile behavior, also considering the polymer thermal properties, and the nanofibers crossings number as a function of the nanofibers diameter. Below a threshold value, which lies between 150 and 250 nm, the overall mat mechanical behavior changes from ductile to brittle, showing enhanced elastic modulus for a high number of nanofibers crossings. While specimen geometry does not affect tensile results. Stress–strain data are analyzed using a phenomenological data fitting model to better interpret the tensile behavior. The experimental results demonstrate the high reliability of the proposed mass-based load normalization, providing a simple, effective, and universally suitable method for obtaining high reproducible tensile stress–strain curves.

1. Introduction

Nonwoven fabrics are structures where fibers are not arranged in a specific pattern (e.g., warp and weft) while still maintaining the aspect and most of the properties of a woven textile. In the form of staple or continuous filaments, the fibers of these materials are kept together by frictional forces through entanglements or adhesive forces between fibers, with or without the use of binders,[1] as a consequence of chemical, mechanical, heat, or solvent treatment. The fibers can be natural or man-made and characterized by any diameter,[1] but usually are in the micrometer range. It is not a simple task to define "nonwovens." Various definitions were proposed (and amended) by different organizations for considering the multifaceted aspects that characterize this class of materials.[2] BS EN ISO 9092:2019 defines nonwoven as "engineered fibrous assembly, primarily planar, which has been given a designed level of structural integrity by physical and/or chemical means, excluding weaving, knitting, or papermaking." As specified by the standard, structural integrity means a "measurable level of added tensile strength," namely the nonwoven should possess some mechanical strength derived from the fiber assembly structure, highlighting the importance of (tensile) mechanical properties.

Nowadays, nonwovens find use in a wide variety of applications, often with high added value, like medical devices, filters, technical clothes, home and industrial furniture, thermal and acoustic insulation, and engineered materials.[3] Several

E. Maccaferri, L. Mazzocchetti, T. Benelli, L. Giorgini
Department of Industrial Chemistry "Toso Montanari,"
University of Bologna
Viale Risorgimento 4, Bologna 40136, Italy
E-mail: laura.mazzocchetti@unibo.it

D. Cocchi, T. M. Brugo, A. Zucchelli
Department of Industrial Engineering
University of Bologna
Viale Risorgimento 2, Bologna 40136, Italy
E-mail: a.zucchelli@unibo.it

D. Cocchi, L. Mazzocchetti, T. Benelli, T. M. Brugo, L. Giorgini, A. Zucchelli
Interdepartmental Center for Industrial Research on Advanced Applications in Mechanical Engineering and Materials Technology, CIRI-MAM
University of Bologna
Viale Risorgimento 2, Bologna 40136, Italy

The ORCID identification number(s) for the author(s) of this article can be found under https://doi.org/10.1002/mame.202100183

DOI: 10.1002/mame.202100183

properties are dependent on the diameter size, such as porosity and pore dimension,[4] which in turn impact, for example, filtering capacity.[4] Mechanical properties, in particular, are significantly enhanced moving from micrometer to nanometer scale.[5] In the last two decades, indeed, nonwoven fabrics made of nanofibers gained increasing attention, thanks to their high surface-to-volume ratio and outstanding properties. Besides the application as highly efficient filters,[6,7] nanofibrous nonwoven mats (known as nanomats too) are successfully used in tissue engineering,[8,9] sensors,[10,11] catalysis,[12,13] and composite materials with enhanced mechanical performances[14–18] and/or peculiar properties.[19] In most applications, the assessment of mat mechanical properties is fundamental for evaluating effective applicability, and tensile testing is commonly performed. However, the highly porous morphology, together with the overall material flexibility and deformability, strongly limit the results reliability and the obtained data cannot be used to design the material for specific applications. Nanofibrous mats are usually very thin and delicate, making them difficult to be handled. Therefore, the specimen preparation for tensile testing requires particular attention for avoiding mat damage, pretensioning, or fibers slipping from the grips during testing. The use of a paper frame to be cut before testing is a valid solution,[20] helping to handle and positioning the specimen, and to better measure the gauge length. However, even when all cautions are taken to run the test, evaluation of the cross-section area, required to normalize recorded load data to calculate the stress (σ), is still troublesome in particular in terms of thickness determination. Indeed, while thickness measurement of nonporous "bulk" materials is simple, it may be tricky for porous and soft ones. Being nanofibrous mats characterized by high porosity, with values close to 90%,[21] the measured thickness is surely affected by the measurement itself. Since nonwovens are very thin and the cross-section area is directly proportional to the thickness, the normalized load values (i.e., stress, σ) may be particularly affected by this drawback. Within this frame, testing of materials is ruled by technical standards published by national and international standards organizations, such as ASTM International, ISO, BSI, UNI, to obtain comparable results. However, there are only a few standards for testing nonwovens, such as ISO 9073 and BS EN 29073, with a lack of specific indications for nanofibrous nonwovens, making them practically not applicable to nanometric fibrous systems. As an example, BS EN 29073-3:1992 (ISO 9073-3:1989), related to the "determination of tensile strength and elongation" of nonwovens, prescribes to prepare a rectangular specimen 50 mm width and, possibly, 200 mm length (gauge length), for "avoiding risks due to local heterogeneity of nonwovens or to undue cutting of long-fiber nonwovens." As a matter of fact, due to the previously discussed difficult handling of nanofibrous mats, the preparation of specimens with these characteristics is practically precluded in most cases. Furthermore, such prescribed specimen size clearly suggests that the considered fibers are not nanometric. It is worth noting that in the cited standard the breaking strength is to be expressed in newtons (N), so actually, it represents the breaking load rather than a "real" strength (σ at break). Again, this is to underline that neither here nor in other standards regarding nonwovens (excluding geotextiles nonwovens[22] and paper,[23,24] which are not considered nonwovens by definition[1]) a method is reported to evaluate the elastic modulus (in MPa) and the strength (load per unit area of cross-section, in MPa) of this type of engineered materials. These tensile properties require σ calculation and, in turn, the evaluation of the mat thickness. The lack of an indication of how to determine tensile properties stems probably from the difficulty in measuring thickness and uniquely defining the thickness. Even if there is a standard for the determination of "conventional" nonwovens thickness,[25] it appears not applicable to nanofibrous nonwovens, since this standard refers to "thicker" nonwovens respect to nanofibrous ones (mm vs μm scale). Besides, the discussed test apparatus is quite complex and not available to common laboratories for routinely procedures. However, the thickness dependency from the applied pressure during measurement surely affects the measured thickness also in "conventional" nonwovens, since BS EN ISO 9073-2 specifies the measuring pressure to be adopted. The standard for paper thickness determination[26] seems not helpful too since the paper is made by cellulose fibers consolidated via pressure during calendering. Consequently, the thickness measurement is less dependent on the measuring pressure, and therefore, the related problem is not as important as in nanofibrous nonwovens. The well-known standard for tensile testing of bulk plastics (ASTM D638) is not useful too.

The mat thickness dependency on the way it is assessed makes it an actual comparison of mechanical performances of nanofibrous nonwovens a difficult task, especially when comparing mats tested by different laboratories. The knowledge of the thickness measurement conditions (mainly the applied pressure) should help, but usually, this information is missing.[9,27–39] The underestimation of this aspect, affecting almost all the studies about tensile testing of nanofibers, prevents any reliable comparison. As a consequence, the state-of-the-art on the topic lacks, despite the widespread growth and use of such nanomaterials.

Presently, a technical standard that establishes a method and the technical criteria to carry out tensile testing of nonwoven nanofibrous mats is not available. To the best of the Authors' knowledge, not even studies concerning data reliability of tensile testing of nanofibrous nonwovens exist. However, given the tremendous boost in the use of nanofibrous nonwovens, searching for a reliable and simple way to tensile test this type of material is of primary importance.

In this work, the Authors present an accurate, systematic, and critical study concerning tensile testing of nonwoven mats, using electrospun Nylon 66 nanofibrous mats as a case study. The "classical" approach to normalization of load by means of specimen cross-section area is compared to a mass-based normalization proposed by the Authors, as well as a normalization based on the mat grammage (areal density). A viable way to convert tensile data of previously tested mats is presented too. Nanofibrous mat characteristics, such as fibers diameter, grammage, and specimen geometry (width and gauge length) are deeply investigated to thoroughly describe the tensile behavior of nonwovens. Mats mechanical performances were discussed considering polymer properties (degree of crystallinity and glass transition temperature), and the number of potential nanofibers crossings as a function of the nanofiber diameter. Experimental stress-strain data are then analyzed using a phenomenological data fitting model to better understand the tensile behavior.

Table 1. Electrospinning process parameters and nanofibers diameters of produced nanofibrous mats.

Nanofibrous mat	Nylon concentration [wt%]	Flow rate [mL h^{-1}]	Electric potential [kV]	Distance [cm]	Electric field[a] [kV cm^{-1}]	Temperature [°C]	Relative humidity [%]	Nanofibers diameter[b] [nm]
Ny150	9	0.30	21.0	7.0	3.0	20–22	25–28	154 ± 38
Ny250	13	0.80	25.0	6.0	4.2	24–26	28–31	256 ± 42
Ny400	18	0.80	25.0	7.0	3.6	20–22	26–28	405 ± 84

[a] Calculated as electric potential to distance ratio; [b] Average values derived from at least 100 diameter measurements on SEM micrographs, manually done on single nanofibers by means of the Photoshop measurement tool.

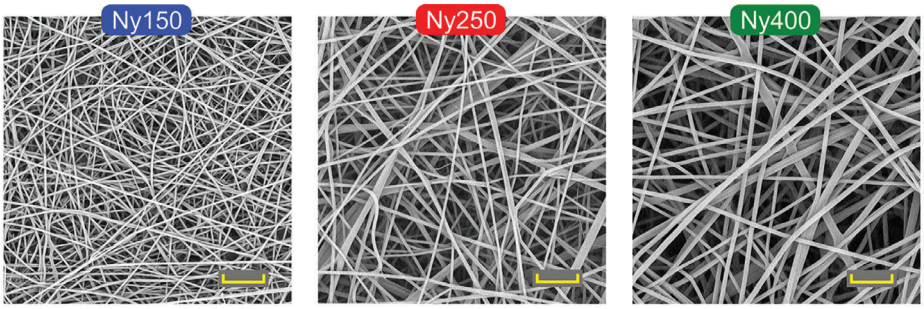

Figure 1. SEM images of the three nanomat types. Scale bar: 4 µm.

2. Experimental Section

2.1. Materials

Nylon 66 (Zytel E53 NC010 kindly provided by DuPont) was dried in a stove at 110 °C for minimum 6 h before use. Trifluoroacetic acid (TFA), formic acid, and chloroform, all reagent grade, were purchased from Sigma-Aldrich and used without further purifications.

2.2. Nylon 66 Solutions and Nanofibrous Mats Production

Nylon 66 solutions having a concentration of 9, 13, and 18 wt% were prepared in a TFA/formic acid/chloroform 10:60:30 vol% (11:55:34 wt%) solvent system. Solutions were made dissolving Nylon 66 pellets under magnetic stirring and mild heating (maximum 50 °C) until complete polymer dissolution.

Nanofibrous mats were produced via electrospinning process, with a Spinbow electrospinning machine unit equipped with four 5 mL syringes (needles 55 mm length and 0.84 mm internal diameter). Fibers were collected on a rotating drum of 150 mm diameter (tangential speed: 0.39 m s^{-1}) covered with poly(ethylene)-coated paper. Mats have final dimensions of approximately 350 × 450 mm and they were labeled Ny*XXX* according to the rough average diameter of the obtained fibers. In **Table 1** electrospinning process and environmental parameters for mats production are reported.

For tensile testing, two nanofibrous mats for each membrane type (Ny150, Ny250, and Ny400) were electrospun for a deposition time one twice the other (dt and 2dt), for a total of six nanomats. Nanofibrous mats for the grammage-thickness relationship assessment were electrospun, picking a membrane strip from the drum (approximately 350 × 60 mm) every 45 min up to 270', obtaining six strips with incremental deposition time (detailed procedure on SI1, Supporting Information).

2.3. Characterization of Nanofibrous Mats and Grammage/Thickness Evaluation

Nanofibrous mats were analyzed by scanning electron microscopy (SEM, Phenom ProX) to determine nanofibers morphology, after gold sputtering. SEM images of the three nanofibrous mat types under analysis are shown in **Figure 1**. Nanofibers diameter, determined measuring at least 50 fibers by an image analysis software, is given as average diameter ± standard deviation in Table 1.

Differential scanning calorimetry (DSC) analyses were carried out on a TA Instruments Q2000 DSC Modulated apparatus equipped with RCS cooling system, calibrated with Indium standard. A sample of 7 mg was heated from 20 °C to 120 °C, cooled to −60 °C, then heated again to 320 °C in nitrogen atmosphere (heating/cooling rate 20 °C min^{-1}).

Tensile tests were carried out using a Remet TC10 universal testing machine equipped with a 10 N load cell, with a crosshead separation speed of 10 mm min^{-1}. Tensile specimens were prepared anchoring the membrane to a paper frame for better handling and avoiding any nanofibers slippage in the machine fixtures, cutting the frame before the test started, as reported before.[20,40] Specimens dimensions are reported in **Table 2**. For each membrane type (Ny150, Ny250, and Ny400) two mats were electrospun, one with a deposition time twice as long as the other (called dt and 2dt). Each tensile specimen is identified by the name of the membrane type (Ny*XXX*) followed by the specimen configuration. Elastic modulus was determined via linear regression of stress-strain data in the strain range 0–1% for all tested specimens (the selection of this specific range was based on the minimization of the linear fitting error).

Table 2. Details of tensile tests specimens (Ny*XXX*: membrane type, i.e. Ny150, Ny250, Ny400).

Tensile specimen configuration	Specimen width (w) [mm]	Specimen gage length (L) [mm]
Ny*XXX*_10/30_dt	10	30
Ny*XXX*_10/30_2dt	10	30
Ny*XXX*_10/45_dt	10	45
Ny*XXX*_10/45_2dt	10	45
Ny*XXX*_20/30_dt	20	30
Ny*XXX*_20/30_2dt	20	30
Ny*XXX*_20/45_dt	20	45
Ny*XXX*_20/45_2dt	20	45

Membranes thickness was evaluated using six different instruments: i) a scanning electron microscope, ii) an analog centesimal indicator, iii) a digital millesimal indicator, iv) an analog millesimal indicator with two different pressure configurations, v) a micrometer and vi) a digital caliper. SEM measurements were carried out on liquid nitrogen fractured mat sections. Details of the resolution and applied pressure by each measurement tool are reported in **Table 3**.

Regarding grammage–thickness relationship, from each membrane strip five patches were extracted (nominally 60 × 25 mm) from different positions along the strip (Figure S2, in SI1, Supporting Information). The mat thickness was measured using the analog indicator 2 in the low-pressure configuration (iv, Table 3), as it allows to compare the measured values with an acceptable resolution. The mat mass was determined using a AS 60/220.R2 Radwag scale with a resolution of 0.01 mg. Detailed description and representation of the adopted procedure are reported in SI1 (Supporting Information). The patch area was evaluated via Matlab software by image processing of scanned images (SI2, Supporting Information).

3. Results

3.1. Membrane Thickness Evaluation and "Classical Approach" to Tensile Test

The accurate evaluation of the thickness is a key factor to characterize several materials properties. This measurement is quite simple when dealing with bulk materials, but it may be very tricky in case of porous and soft materials, since the measurement procedure itself affects the measured thickness value. Nonwovens, to which electrospun nanofibers clearly belong, are surely affected by this drawback. To demonstrate it, two Ny250 membranes, named Ny250_dt and Ny250_2dt, were electrospun for a deposition time one twice the other (dt and 2dt), to assess the thickness of each membrane, evaluated in a limited area, where the nanofiber deposition is expected to be homogeneous. The histograms in **Figure 2**A show the thickness measured on the two different Ny250 membranes using the measurement tools reported in Table 3.

The measured thickness is strongly affected by the tool used for its evaluation, resulting in very different values, with a maximum observed discrepancy of about 300% within the same area. It can be surely affirmed that overall Ny250_dt mat is thinner than Ny250_2dt (provided that the comparison is done using the same instrument), but it is not possible to define the mat thickness uniquely, as the measurement tool influences the recorded value as a function of the applied pressure.

The use of different thickness values may, in turn, affect enormously tensile test results. The recorded load–displacement data, which do not consider the dimensions and geometry of the specimen, require normalization to obtain comparable stress–strain curves. The classical approach used for stress evaluation (σ, in MPa) requires the specimen thickness (t, in mm) for evaluating the cross-section area (S, in mm^2) normal to the applied load direction, as shown by the following equation:

$$\sigma = \frac{F}{S} = \frac{F}{wt} \tag{1}$$

where F is the force N and w the specimen width mm. Clearly any variation in t significantly affects σ, being the section S directly proportional to it.

Tensile tests were performed on two specimens with a dimension of 20 × 45 mm sampled from the analyzed region of Ny250_dt and Ny250_2dt. For each specimen, stress values were calculated according to Equation (1) using the thicknesses reported in Figure 2A, obtaining the multiple stress-strain curves represented in Figure 2B. The curves display significantly different profiles, while they should be in principle overlapped or, at least, highly resembling one each other. As a consequence, both elastic modulus (E) and maximum stress (σ_{max}) assume completely different values, ranging from 35 to 100 MPa and

Table 3. Technical specifications of measurement tools used for evaluating membranes thickness.

Instrument	SEM	Analog indicator 1	Digital indicator	Analog indicator 2	Analog micrometer	Digital caliper
Type of measurement	Electron microscopy	Mechanical	Mechanical	Mechanical	Mechanical	Mechanical
Producer	Phenom ProX Phenom World Netherlands	Borletti Italy	Alpa MegaRod Italy	Borletti Italy	Holex Germany	Alpa Italy
Resolution	≤8 nm	10 µm	1 µm	1 µm	10 µm	10 µm
Pressure	n.d.	83 g cm^{-2}	94 g cm^{-2}	Low config. 360 g cm^{-2} High config. 1062 g cm^{-2}	Depending on operator	Depending on operator
Color identification				Low config. High config.		

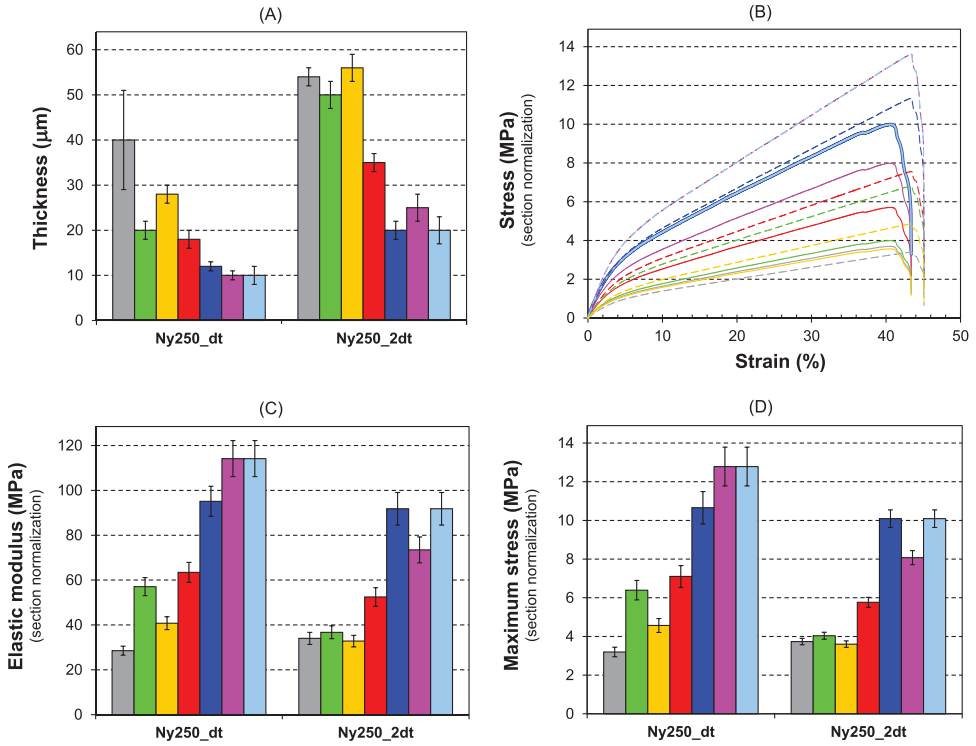

Figure 2. A) Thickness measurements on the two distinct Ny250 nanofibrous mats, using different measurement tools. B) Comparison of stress-strain curves of the tensile tests performed on Ny250_dt (dashed lines) and Ny250_2dt (solid lines) obtained from the application of the "classical approach" as per Equation (1), using the different thicknesses reported in (A). C) Elastic modulus and D) maximum stress derived from the analysis of stress-strain curves in (B). The colors are coherent with the ones adopted for the identification of the measurement instruments (see Table 3).

4–14 MPa, respectively (Figure 2C,D). It is, therefore, demonstrated that the thickness measurement methodology deeply affects the results. Moreover, it is worth mentioning that even using the same tool, different stress-strain curves are obtained for the two considered specimens, though in theory the result should be the same. Indeed, the lower the thickness of the nanofibrous mat to be measured, the greater the relative error, since the dimension of the mat is evaluated as the difference between the overall thickness of the mat and the supporting paper minus the one of the papers alone.

Such scattered results are obviously unacceptable, pointing at the impossibility of making any reliable comparison of nanofibrous mats tensile properties made by different research groups. Curves can be reliably compared only within the same type of nanofibrous mats measured with the same instrument and in the same conditions. Nonetheless, even under these assumptions, stress–strain curves may not be comparable when dealing with "extremely low" thickness, as the measurement error compares to the actual measurement value. E and σ_{max} should, instead, be unaffected by the particular specimen geometry, being these values characteristics of the material. Finally, beside all the above considerations on the correct thickness evaluation, an additional issue arises when trying to follow Equation (1), since the nanofibrous mat is wrongly considered as a bulk material: the voids among nanofibers are assumed to be filled by the polymeric material, leading to a significant underestimation of σ and of all related properties.

3.2. Tensile Test Data Normalized with Respect to Nanofibrous Mat Grammage

A general, simple, and reliable method to normalize the load–displacement data for obtaining more comparable stress-strain curves is highly needed. The use of nanofibrous mat grammage (G, in g m^{-2}, defined as per Equation (2)), which involves the mat mass measurement and its surface area (A, in m^2), may be a viable solution. Hereafter mathematical steps are reported to express stress (σ, in MPa) as a function of grammage (Equation (3)).

$$G = \frac{m}{A} = \frac{m}{L\,w} \tag{2}$$

$$\sigma_{eq} = \frac{F}{S_{eq}} = \frac{F}{w\,t_{eq}} = \rho_m \frac{F}{G\,w} \tag{3}$$

where σ_{eq} (in MPa) is the stress "equivalent" to a specimen with the same dimensions (length, L and width, w, both in m) and mass (m, in g), but condensed in a bulk film characterized by equivalent thickness t_{eq} (in µm), volume V_{eq} (in cm^3), and cross-section area S_{eq} (in mm^2); ρ_m is the density (in mg mm^{-3}) of the material used to manufacture the nanofibers (1.14 mg mm^{-3} for Nylon 66). Applying Equation (3) to the previously discussed Ny250_dt and Ny250_2dt mats, the resulting stress–strain curves are now closer each other (**Figure 3**).

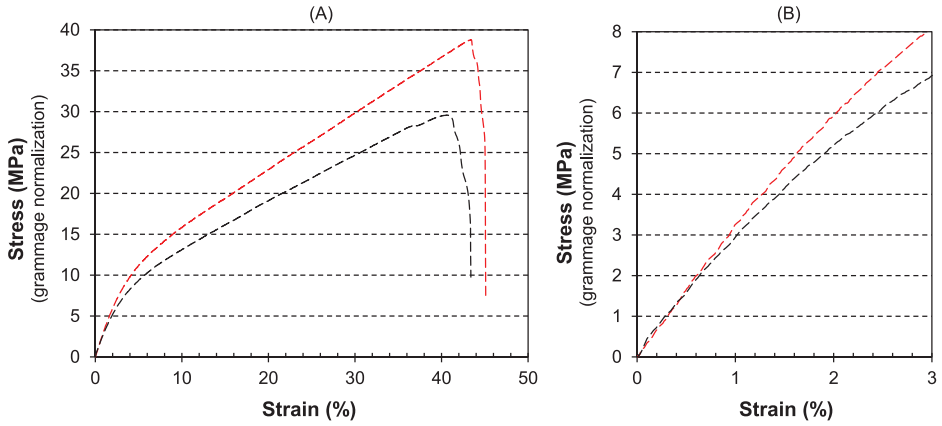

Figure 3. A) Stress–strain curves of the two specimens sampled from Ny250_dt (in red) and Ny250_2dt (in black) mats, obtained following load data normalization based on membrane grammage (Equation (3)). B) Enlargement of the stress–strain curve in the low deformation range (0–3%).

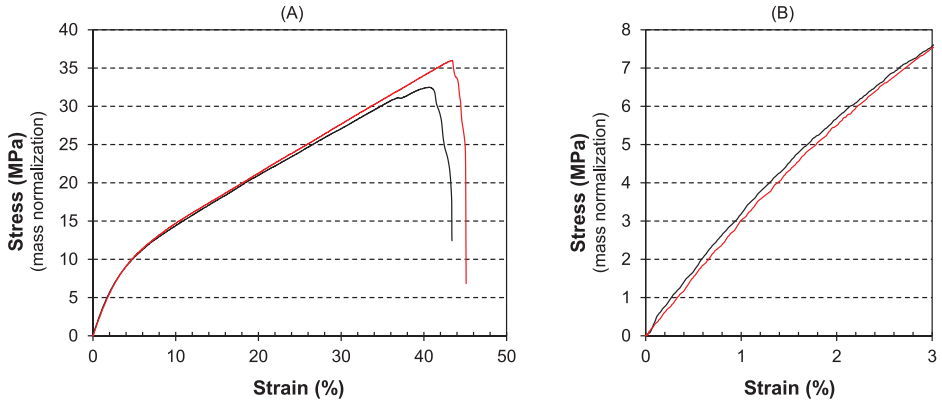

Figure 4. A) Stress–strain curves of the two specimens sampled from Ny250_dt (in red) and Ny250_2dt (in black) mats, obtained according to load normalization based on specimen mass (Equation (4)). B) Enlargement of the stress–strain curve in the low deformation range (0–3%).

This stress normalization method, however, suffers from some drawbacks too. Indeed, the application of Equation (3) presumes that the mat grammage is constant across the entire membrane area from which the tensile specimens are sampled out. This assumption, though, may not be true because of the nanofibers additive deposition typical of the electrospinning process, which could lead to local inhomogeneities in fibers distribution. Besides, the grammage evaluation needs a certain amount of material and several measure repetitions to obtain reliable values.

3.3. Tensile Test Data Normalized with Respect to Specimen Mass

Using the specimen mass for the load–displacement data normalization, instead of the overall mat grammage, allows for a better match of the recorded load values with the tested specimen, resulting in reliable and absolutely comparable stress-strain curves, as shown in **Figure 4**. Hereafter equations are reported to explain the relationship between stress and specimen mass (Equation (4)):

$$\sigma_{eq} = \rho_m \frac{F}{G\,w} = \rho_m \frac{F}{w}\frac{L\,w}{m} = \rho_m \frac{F}{m} L \tag{4}$$

In this case, the behavior of the two tested specimens looks utterly comparable: the stress–strain curves are almost superimposed, with a little deviation only at high strain values, in the final nonlinear segment of the curve, where nanomat failure occurs. The differences in the maximum stress are due to the specimens failure mode, usually unpredictable due to peculiar imperfections.

By applying this normalization method, it is therefore possible to obtain perfectly reliable and repeatable results, similarly to what happens for bulk materials. A direct comparison between the load normalization based on mat grammage and on specimen mass (according to Equations (3) and (4), respectively) is reported in **Figure 5**. The graph shows that the use of nanomat grammage for load normalization is less reliable and less convenient than the specimen mass normalization, though it allows to renormalize tested specimens whose mass is unknown. Whether the specimen mat grammage nor the nanomat from which the specimens were obtained are unavailable, it is possible to assess the grammage via the linear grammage-thickness relationship, as later demonstrated. Although the grammage normalization of the load is less reliable respect to the mass one, it nevertheless appears better than the "classic" normalization approach based on the specimen cross-section area.

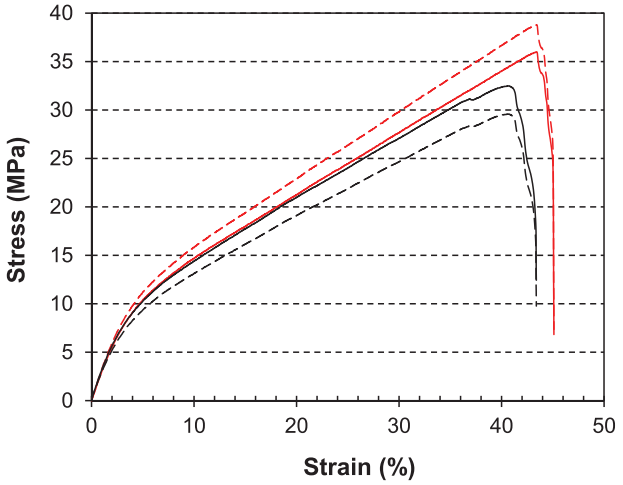

Figure 5. Comparison of stress–strain curves of the two specimens sampled from Ny250_dt (in red) and Ny250_2dt (in black) mats, obtained according to load normalization based both on mat grammage (Equation (3)), dashed lines) and on specimen mass (Equation (4), solid lines).

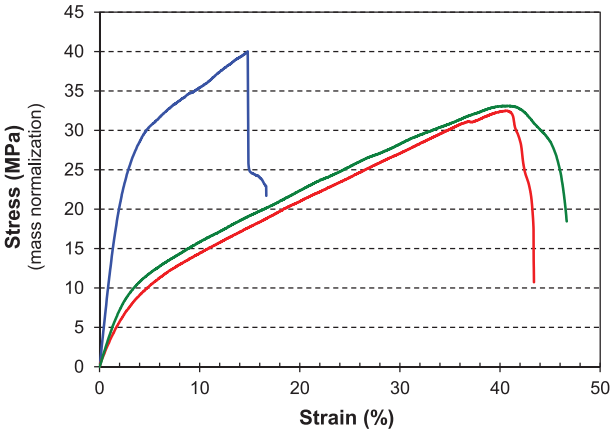

Figure 7. Representative stress–strain curves of the three different membrane type (Ny150 blue, Ny250 red, and Ny400 green). The displayed specimens were selected from the 20/45_2dt configuration.

Figure 6 shows the comparison between the different approaches to load-displacement curve normalization, reporting for each one its pros and cons.

3.4. Nanomats Tensile Tests Analysis

In this section, the mass normalization approach has been applied to the analysis of tensile tests carried out on different tensile specimen configurations (Table 2). **Figure 7** shows the representative stress-strain curves of the three different membrane types (Ny150, Ny250, and Ny400), while the curves for all the specimen configurations are shown in SI3 (Supporting Information). At first glance, the mechanical behavior of Ny150 mat is completely different from the other two, which are, instead, very similar. The analysis of these curves will be discussed in detail in the next Sections.

3.4.1. Effect of Specimen Geometry

Load–displacement curves are characteristic of each specimen, as they are size dependent. To remove the dependence on geometry, it is necessary to consider the stress-strain curves, which allow characterizing the intrinsic mechanical properties of the material. To evaluate a possible dimensional effect on the mechanical characteristics, for each membrane type several specimens with different dimensions (width, length, and grammage, Table 2) were tested. **Figure 8** shows the elastic modulus and the maximum stress for the specimens obtained from the membrane Ny250_dt and Ny250_2dt, normalized both

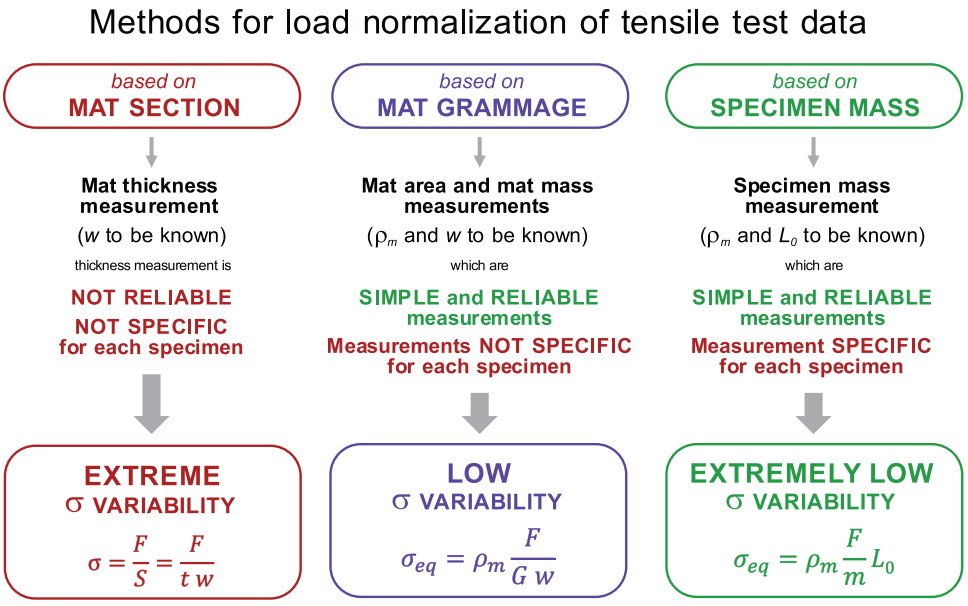

Figure 6. Comparison between the different approaches to load normalization.

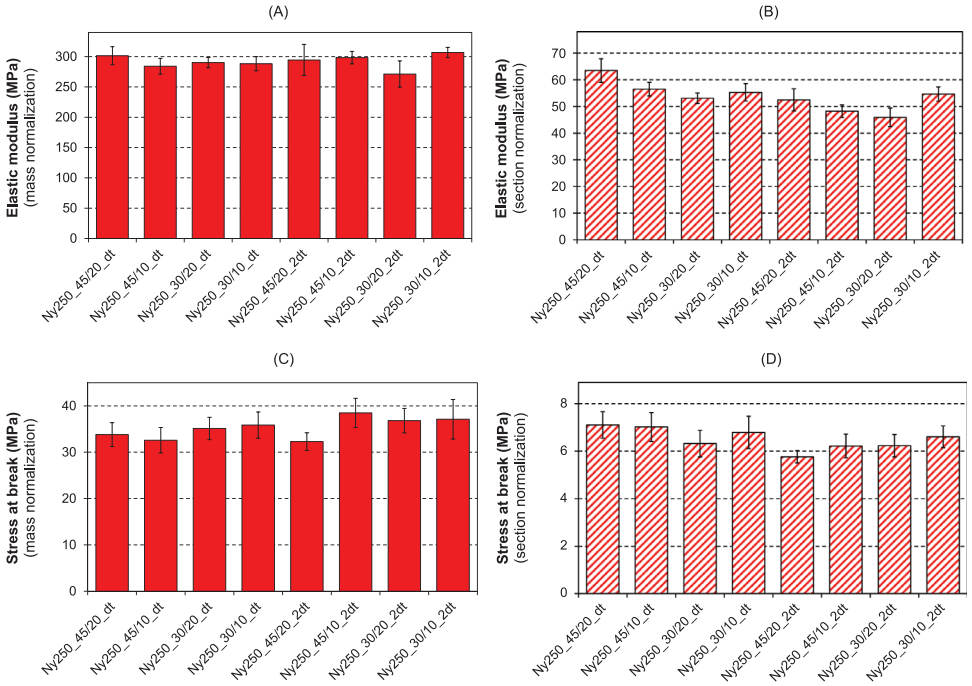

Figure 8. Elastic modulus and maximum stress for the specimens obtained from the membrane Ny250_dt and Ny250_2dt, normalized both on mass (A and C respectively, solid filling) and on cross-section area (B and D respectively, dashed filling).

on mass (A and C, respectively) and on section (B and D, respectively).

Data from Figure 8 show that the size of the specimens does not significantly affect both the elastic modulus and the maximum stress. The dramatic differences in numerical values between the two normalization methods are due to the inaccuracies of the section normalization method. Indeed, the thickness measurement, besides not being reliable, also considers the voids inside the nanomat as actively contributing to its response to the tensile stimulus, accounting for a fictitious far larger cross-section area than the actual one bearing the load. On the contrary, the mass-based load normalization discards the voids contribution, considering the mat specimen a bulk material characterized by the same length, width, and mass, with the exception of the thickness (t_{eq}), and still maintaining the nanofibrous morphology. Similar results were also observed for the Ny150 and Ny400 mat types (histograms are reported in SI4, Supporting Information). The results derived from grammage-based load normalization are not presented here because the aim is to compare the effectiveness of the proposed mass-based normalization method with the commonly adopted approach based on section normalization.

3.4.2. Effect of Nanofiber Diameter

To evaluate the effect of the nanofiber diameter on the mechanical properties of the nanomat, three different types of membranes were electrospun, each characterized by different nanofibers diameter: 150, 250, and 400 nm (Ny150, Ny250, and Ny400, respectively). The histograms show for each specimen configuration the elastic modulus (**Figure 9**A), maximum stress (Figure 9B) and strain at maximum stress (Figure 9C). Elastic modulus and maximum stress derive from the mass-based load normalization.

The tensile properties of each mat type, averaged regardless of the specimen geometry, are collected in **Table 4**.

The Ny150 membrane type, characterized by a significantly higher elastic modulus than the other two mat types (about three times), is more rigid and consequently displays a more brittle behavior, with a strain at maximum stress ($\epsilon_{\sigma max}$) about 1/3 and a halved toughness (U) respect to Ny250 and Ny400. E, σ_{max}, and $\epsilon_{\sigma max}$ values of the Ny250 and Ny400 membranes are almost comparable, as well as the toughness. It is worth to mention that Ny250 and Ny400 mats show a ductile behavior, while Ny150 exhibits a more brittle one, as can be also observed from stress-strain curves of Figure 7.

Two main reasons may be given for explaining the different mechanical behavior among the mat types: i) a difference in the polymeric material, such as a variation of the Nylon 66 degree of crystallinity, and ii) an effect related to the nanofibrous mat morphology, like the number of nanofibers intersections.

The Nylon ability to crystallize may be affected by the processing conditions, which could lead to different average size of the crystallites and/or affect the degree of crystallinity.[20] Electrospun Nylon 66 nanofibers may change their degree of crystallinity, as well as the "quality" of the crystallites, depending on the electrospinning solution solvent system,[5,41] the presence of nano-reinforcements like graphene which may act as nucleant,[20] and the nanofiber size.[5] According to Baji et al.,[5] the fiber diameter strongly affects mechanical properties, resulting significantly enhanced below a threshold diameter, which in

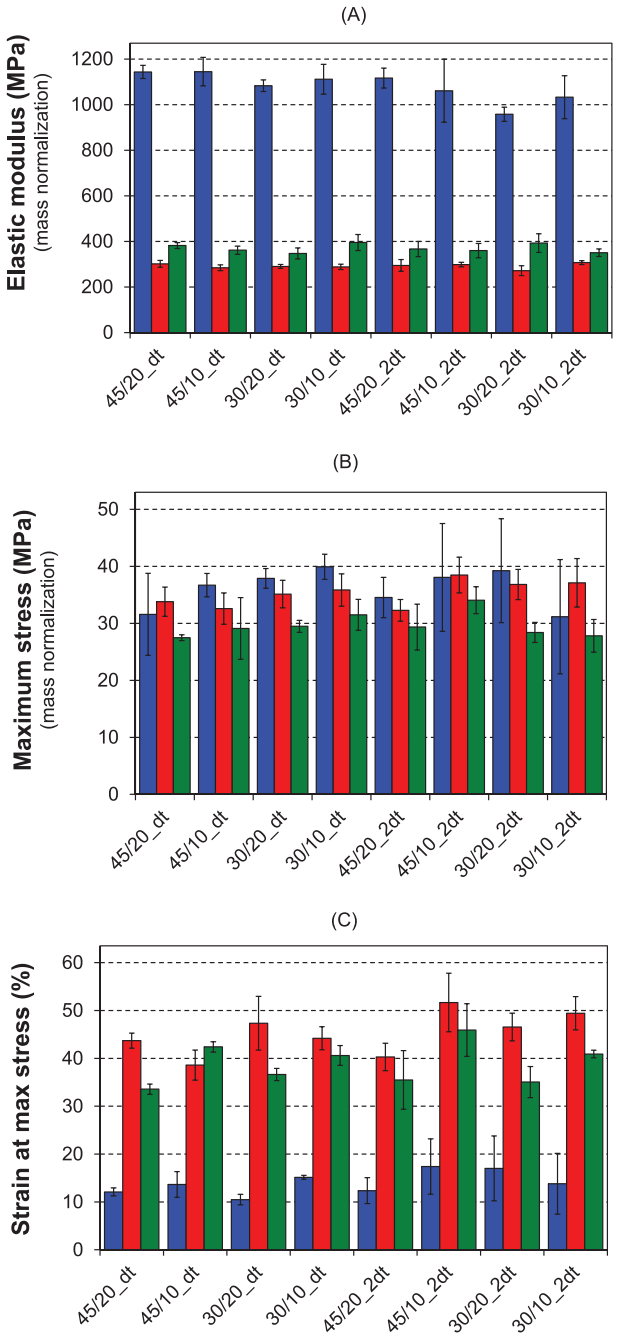

Figure 9. A) Elastic modulus, B) maximum stress and C) strain at maximum stress for each specimen configuration reported in Table 2. In blue Ny150 specimens, in red Ny250 specimens and in green Ny400 specimens.

their case was near ≈500 nm for Nylon 66 nanofibers electrospun from a formic acid/dichloromethane solvent system. The nanofibers under study in the present work, especially Ny150 and Ny250, are clearly below this value. Tensile tests, however, show a significant increment of elastic modulus and strength only for nanofibers with the smallest diameter (150 nm), while thicker fibers mats behave alike. In this context, it is worth mentioning that in the cited work[5] Nylon 66 nanofibers were aligned, while in the present case the tested nanofibers are randomly oriented, so the two cases cannot be straightforwardly compared. The nanofibrous mats were thus investigated via DSC analysis to evaluate the effect of the nanofiber morphology on the Nylon 66 thermal properties, which may contribute to the observed different mechanical behavior of the nanomats (**Figure 10**).

As expected for a semicrystalline polymer, the thermograms show a stepwise variation of the thermal capacity ascribable to the polymer glass transition and an endothermic signal accounting for the melting of the polymer crystalline fraction. All the mats have a similar degree of crystallinity ($\chi_c \approx 45\%$), even if some differences on peaks shape and positioning were observed. Also the glass transition temperatures (T_gs) show slight differences, which are, however, not enough to justify the utterly different mechanical behavior. Indeed, the observed T_gs are almost comparable, with only a slightly higher value for the Ny150 (69 °C vs 64 °C and 65 °C of Ny250 and Ny400, respectively), accounting for a possible slightly higher orientation of the Nylon 66 amorphous phase of Ny150 mat. Detailed explanation of DSC analysis regarding degree of crystallinity evaluation and melting peaks interpretation is reported in SI5 (Supporting Information).

Since the mats thermal behavior are well comparable, it was investigated whether there is an influence of the nanofibrous morphology on the mechanical properties, particularly the number of intersections between nanofibers (crossings). These can be, for example, localized weldings between nanofibers, electrostatic connections, slipping-resistance points. The knowledge of number and type of intersections, in fact, would be extremely important to interpret the mechanical behavior of a random nanomat at the macroscale. While it is very difficult to establish the type of intersections, their numeric estimation is certainly more viable. Since for the three types of membranes considered both the electrospun polymer and the solvent system are the same, and the electrospinning conditions are very similar (especially potential, distance, and hence electrostatic field), it can be assumed that the quality of the fiber bonding at the contact points is comparable. In particular, it is known that the needle-to-collector distance (affecting both the time of flight of the polymeric jet and the evaporation rate of the solvent) is the parameter that can most affect the quality of fiber bonding.[46] Besides, this aspect is also supported by the fact that the DSC analysis does not show differences in glass transition temperature nor in degree of crystallinity on Nylon 66, resulting in the observed increase in mechanical properties of Ny150. Hence, the different tensile behavior observed does not arise from a substantial difference in the material.

Different software for image analysis can be adopted for the quantification of the nanofibers crossings. However, from SEM micrograph it is impossible to correctly assess the number of intersections through the entire thickness. To this end, an alternative and easy-to-apply method has been adopted. Several approaches have been proposed to estimate the number of crossings per unit area of stochastic fibrous networks.[42–44] Assuming the nanofibers as infinite length lines, it is possible to model the random mat as a network of lines crossing in points distributed according to a point Poisson process in the plane.[43] As reported in ref. [44], the expected number of crossings per

Table 4. Average tensile properties for each membrane type.

Membrane type	E [MPa]		σ_{max} [MPa]		$\epsilon_{\sigma max}$ [%]		U [J cm^{-3}]	
	Mean ± SD	CV [%]	Mean ± SD	CV [%]	Mean ± SD	CV [%]	Mean ± SD	CV [%]
Ny150	1071 ± 90	8	36 ± 7	19	13 ± 5	38	4.0 ± 1.5	38
Ny250	296 ± 28	9	35 ± 3	9	46 ± 6	13	9.4 ± 1.3	14
Ny400	355 ± 37	10	30 ± 4	13	39 ± 6	15	7.8 ± 1.8	23

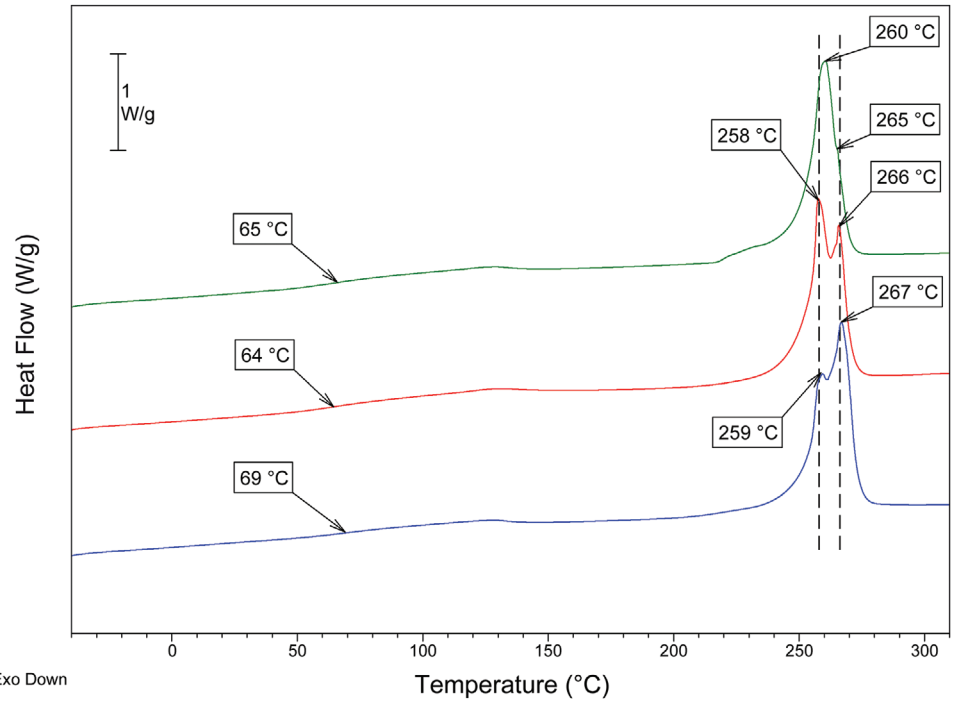

Figure 10. DSC analysis of the three membrane types (Ny150 blue, Ny250 red, Ny400 green).

unit area (n_c^{fibers}) depends only on the total fibers length per unit area (τ, in m^{-1}):

$$n_c^{fibers} = \frac{\tau^2}{\pi} \tag{5}$$

Assuming a nanofibrous sample consisting of a single continuous cylindrical filament, with an average diameter d, it is possible to estimate its equivalent length (l_{eq}) starting from its volume ($V_{filament}$) by the following steps:

$$l_{eq} = \frac{4m}{\rho_m \pi} \frac{1}{d^2} \tag{6}$$

where τ is defined as the l_{eq} per unit area (m m^{-2}). It should be noted that Equation (5) is true only in the case of 2D networks, as it is assumed that each crossing generates contact between nanofibers. The nanofibers of real networks, instead, may or may not contact each other, depending on the influence of nearby nanofibers. However, considering only 1 g of nanofibers randomly distributed on a 1 m^2, it is reasonably possible to assume that Equation (5) holds true. By replacing Equation (6) in Equation (5), it is possible to estimate n_c^{fibers}, knowing only the mass of the mat (m), the density of the electrospun material (ρ_m), and the average diameter of the nanofibers (d), obtaining:

$$n_c^{fibers} = \frac{16m^2}{\rho_m^2 \pi^3} \frac{1}{d^4} \tag{7}$$

Figure 11 shows, for each nanomat type, the equivalent filament length (l_{eq}) and the number of crossings per unit area (n_c^{fibers}) considering a unitary grammage.

It is interesting to note that l_{eq} is inversely proportional to the square of its diameter (Equation (6)), so nanofibers with smaller diameters determine a higher potential number of intersections. By plotting the number of crossings as a function of the nanofiber diameter in a log–log scale, a linear trend can be observed. Knowing the average value of the nanofiber diameter, it is possible to estimate the n_c^{fibers} for different nanomats, provided the same material is used. It can be observed that the calculated crossing number for the Ny250 and the Ny400 mats are 87% and 98% lower than the Ny150 one, respectively. Given the high difference in the number of n_c^{fibers} that characterize each nanomat,

Nanofibrous mat	d [nm]	l_{eq} [m]	var. [%]	n_c^{fibers} (a) [m^{-2}]	var. [%]
Ny150	154	4.7E+07	–	7.1E+14	–
Ny250	256	1.7E+07	-64%	9.3E+13	-87%
Ny400	405	6.8E+06	-86%	1.5E+13	-98%

[a] evaluated on an area of 1 m^2 for a 1 g of nanofibers (unitary grammage)

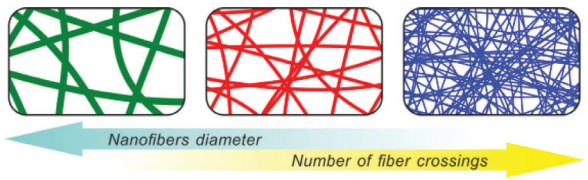

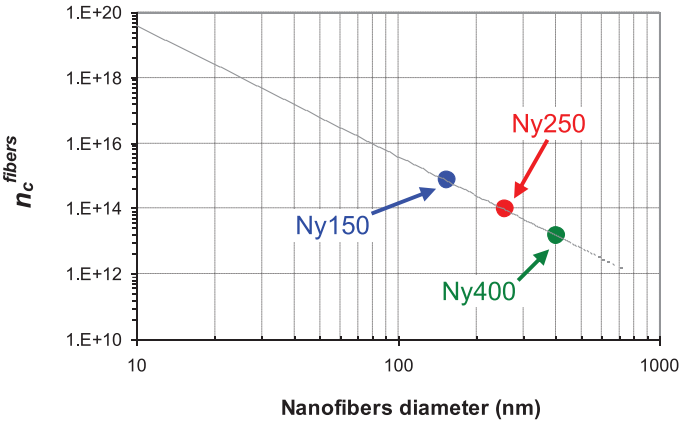

Figure 11. Equivalent filament length (l_{eq}), number of nanofibers crossings per unit area (n_c^{fibers}) and its plot versus nanofibers diameter (d).

it can therefore be assumed that the changes in mechanical behavior are mainly ascribable to this aspect. A similar result was also observed in a numerical study on the mechanical characterization of 2D fibrous networks.[45] As shown in Table 4, elastic modulus, strain at maximum stress and toughness values of Ny150 mat are substantially different from those of Ny250 and Ny400 membranes, which instead do not diverge significantly in between each other. Therefore, it can be supposed that there is a threshold value of the nanofibers diameter, in the range 150–250 nm, that leads to a substantial change in the macroscale mechanical behavior, and it can be hypothesized that the number of nanofibers crossings is also connected to this aspect. For a high number of crossings (in the case under investigation more than 10^{14} for unitary grammage), indeed, the mechanical properties are higher and the behavior more brittle.

For the above considerations, it seems acceptable to attribute the different mechanical behavior of the Ny150 to the significant difference in the number of nanofibers crossings compared to the other two membranes under study. It is to remark that the crossings estimation, as well as the application of the data fitting model explained in the next subsection, are applicable only for random fibrous networks and not for aligned fibrous mats.

3.4.3. Application of the Phenomenological Data Fitting Model

Tensile stress–strain curves of mats with randomly oriented fibers have a peculiar shape, which displays a nonlinear trend followed by a linear one, as largely found in the literature.[20,28,33–36,39,40,47–50] The tested mats show this behavior too: the stiffness decreases from an initial value down to an asymptotic constant trend for high strains. In particular, the mechanical behavior is characterized by three main stages: an initial nonlinear trend (Stage I), followed by a linear one (Stage II), and finally an additional nonlinear behavior where the stress reaches a maximum value before mat failure (Stage III). To better understand the phenomena, the Authors developed, and already successfully applied,[20,40] a data fitting model. The calculated stress (σ) can be expressed as the superimposition of two stress contributions: a linear one (σ_1) and a nonlinear one (σ_2), formulated as in the following equation:

$$\sigma(\varepsilon) = \sigma_1(\varepsilon) - \sigma_2(\varepsilon) = (a\varepsilon + b) - (be^{-c\varepsilon}) = a\varepsilon + b(1 - e^{-c\varepsilon}) \quad (8)$$

where a, b and c are parameters experimentally determined to obtain the data fitting. In the present work, the solver tool implemented in Microsoft Excel was used for minimizing the sum of square error (method of least squares).

In **Figure 12**A, the comparison between the experimental stress-strain curve and the data fitting curve is shown for Ny250 mat (Ny250_20/45_2dt), as well as the average data fitting parameters resulting from the application of Equation (8) to all the tested specimens (in the SI6, Supporting Information other examples of data fitting are presented).

While the common analysis of stress–strain curves involves, mainly, the determination of Young's modulus and the properties at break, the use of the present data fitting model allows to thoroughly analyze the mechanical behavior of the nonwoven mat.

The elastic modulus is commonly expressed as the slope of the tangent to the stress-strain curve at a low strain. This approach was applied for the elastic modulus calculation in Sections 3.4.1 and 3.4.2, and in SI4 (Supporting Information), by means of the linear regression of the stress–strain data at the early strain stage (0–1%). However, the mat is characterized by a nonlinear trend and a subsequent linear one, as clearly displayed in Figure 12A. The linear trend, which appears at "higher" strains, should also be considered for a thoroughly evaluation of the mat tensile properties.

By deriving the stress, as expressed in Equation (8), respect to the strain, the following relation represents the slope of the tangent to the stress–strain curve:

$$\frac{d\sigma}{d\varepsilon} = E(\varepsilon) = a + bce^{-c\varepsilon} \quad (9)$$

where $E(\epsilon)$ describes the local material stiffness as a function of the strain. This relation is useful for evaluating the mat stiffness at very low (for $\epsilon \to 0$) and at very high (for $\epsilon \to \infty$) strains, allowing to define an initial mat stiffness (or initial Young's modulus, E_0, Equation (10)), and an asymptotic constant stiffness (or the

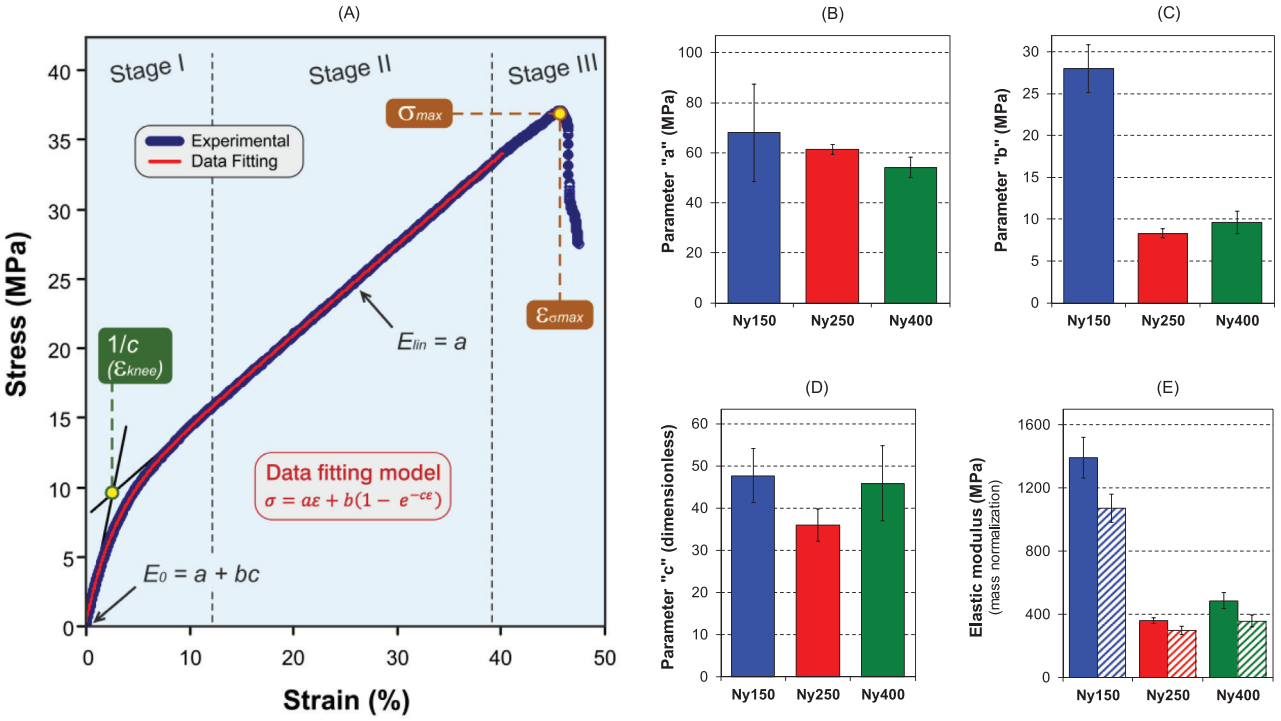

Figure 12. A) Application of the data fitting model to Ny250_20/45_2dt stress–strain curve. B–D) Average data fitting parameter for Ny150 (blue), Ny250 (red), and Ny400 (green) mats. E) Comparison between E_0 calculated as per Equation (10) (solid colors) and the elastic modulus calculated as the slope of the tangent to the stress–strain curve (dashed).

Young's modulus of the linear trend of stress–strain curve, E_{lin}, Equation (11)):

$$E_0 = \lim_{\varepsilon \to 0} E\ (\varepsilon) = a + bc \tag{10}$$

$$E_{lin} = \lim_{\varepsilon \to \infty} E\ (\varepsilon) = a \tag{11}$$

Therefore, the mat is characterized by two elastic moduli, E_0 and E_{lin}, accounting for two distinct material behaviors. E_0 is shown in Figure 12E, as well as the elastic modulus calculated as the slope of the tangent to the stress-strain curve (same data in Table 4) for the sake of comparison. E_{lin} values, corresponding to a parameter, are shown in histograms of Figure 12B.

The elastic moduli calculated with the two approaches show a similar trend, but are different in absolute values: on average, E_0 is from one fourth (Ny250) to one third (Ny150 and Ny400) higher than the "classically" determined elastic modulus. This discrepancy can be explained considering the nonlinear trend displayed by the stress–strain curve in Stage I. At a first look, the curve seems to have an initial "linear" trend and, consequently, a proportional limit within the Hooke's law ($\sigma = E \bullet \epsilon$) is valid. Deep focus on the curve shows that no Hookean region is detectable, not even for low strains as the range considered for the slope determination (0–1%). Indeed, the mat local stiffness lowers progressively, as clearly evidenced by the trend of $E(\epsilon)$. E_0, being the extrapolation of the mat elastic modulus at null strain (for $\epsilon \to 0$), has a higher value respect to any other elastic modulus value calculated by the slope tangent method. Consequently, E_0 should be considered a "theoretical" elastic modulus. Nonetheless it may be useful to obtain a value which is operator-independent, contrarily to the slope tangent method which suffer from the specific strain range considered.

According to Equations (10) and (11), E_0 and E_{lin} are only functions of the parameters a, b, c, therefore their deeper analysis may help to interpret the mat mechanical behavior. The comparison of the experimental parameters (Figure 12B–D), averaged from the data obtained from all the tested specimen geometries, highlights a significant difference in the b parameter of Ny150 (28 ± 3 MPa) respect to Ny250 and Ny400, that are statistically comparable (8.3 ± 0.5 and 9.6 ± 1.4, respectively). The other two parameters, a and c, seem to be unrelated to the geometrical/morphological factors of the nanofibrous mat.

The a parameter, as declared by Equation (11), represents the mat elastic modulus in the linear trend at high strain (Stage II). The obtained values are comparable for all the mat types (54–68 MPa). In that region the membrane already underwent large deformations: as a result the fibers, still random at a nanoscale level, are growing oriented in the direction of the applied load. In these conditions, the resulting stiffness should be mostly related to the intrinsic mechanical properties of the material, regardless of its morphology. The a mean value, irrespective of the standard deviation, becomes slightly lower as the diameter increases: this may be attributed to the different mechanical properties derived by the differences of the polymer crystallites "quality," as highlighted by DSC analysis (Section 3.4.2 and SI5, Supporting Information). The high standard deviation of the a parameter in Ny150 (coefficient of variation of 29%, respect to 3% and 8% for Ny250 and Ny400, respectively) stems from the troubles in

applying the data fitting model to mats with brittle behavior, which do not display a sufficient linear trend extension (Stage II).

The b parameter is involved in both σ_1 and σ_2 (Equation (8)), but its contribution is different depending on the strain region considered. At very low strains (for $\epsilon \rightarrow 0$), both σ_1 and σ_2 converge to b value. While, at high strains, σ_1 and σ_2 are partially affected by this parameter. Consequently, the b impact on the resulting $\sigma(\epsilon)$ is significant in Stage I (nonlinear region), where b acts as a multiplier of the exponential $e^{-c\epsilon}$. σ_2 describes how rapidly the stress–strain curve deviates from the linear trend at low strains.

The c parameter refers to the region where the stress–strain curve change slope from the E_0 value to the E_{lin} one. More specifically, $1/c$ represents the onset extrapolation of the slope change (ϵ_{knee}), as can be derived from Equations (10) and (11) reported in ref. [40]. Ny150 and Ny400 have a similar average c (48 and 46, respectively) which corresponds to $\epsilon_{knee} = 0.0021$, while Ny250 has $c = 36$ and consequently a higher ϵ_{knee} (0.0028). All the c values are statistically comparable, nonetheless. This parameter affects only σ_2 and, similarly to b, contributes to $\sigma(\epsilon)$ via the exponential term.

Since a significant difference is found only for b parameter (for Ny150 mat is three times higher), it is possible to assume that this parameter is related to the morphology of the nanofibrous mat, and in particular to the number of intersections. It is interesting to note that the same trend has been found for the experimental elastic modulus (Figure 9A and Table 4).

3.5. Grammage-Thickness Relationship for Grammage Renormalization of Load–Displacement Curves

Finally, with the aim to characterize nanofibrous mats not only mechanically but also morphologically, a study was carried out to assess whether there is a relationship between the thickness and the grammage of a nanomat. This relationship is easily predictable for bulk materials, but it is not for nonwoven fabrics, and particularly for electrospun nanomats, which contain a high fraction of voids. Moreover, this analysis is useful for the grammage renormalization of load-displacement curves previously normalized on the cross-section area, for which only the thickness of the mat is known. To this end, for each membrane type, thickness, weight, and area (and therefore grammage) of the nanofibrous patches were assessed (detailed description in Sections 2.2 and 2.3 and in SI1 and SI2, Supporting Information). At this stage, only one instrument was used for thickness assessment to obtain comparable measurements. The instrument used is the analog indicator 2 in the low-pressure configuration (iv, Table 3), as it allows to compare the measured values with an acceptable resolution. In the following equations, the steps to obtain the relationship between the grammage G and the thickness t of the nanomat are reported. By knowing the density ρ_m of the electrospun material, it is possible to express the mass m of the mat as a function of the fiber volume V_f ($m = \rho_m V_f$). Furthermore, the percentage fiber volume $V_{f\%}$ can be expressed as the ratio between the fiber volume V_f and the total volume V of the mat:

$$V_{f\%} = \frac{V_f}{V} = \frac{V_f}{L\,w\,t} \tag{12}$$

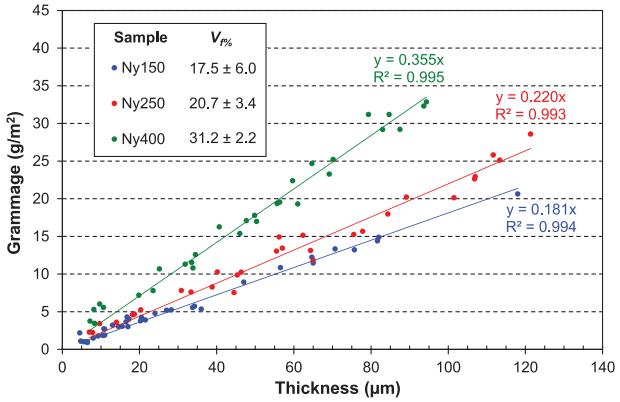

Figure 13. Grammage-thickness plot. The colored dots represent the experimental measurements, while the regression lines represent the calibration lines for each type of membrane (Ny150, Ny200, and Ny400).

where L, w and t are the length, width, and thickness of the nanomat. According to Equation (2), concerning the grammage G of the nanofibrous mat, and replacing the previous equations, it can be proven that:

$$G = \frac{m}{L\,w} = \frac{\rho_m V_f}{L\,w} = \frac{\rho_m V_{f\%} L\,w\,t}{L\,w} = \rho_m V_{f\%}\,t \tag{13}$$

Equation (13) clearly displays the linear relationship between grammage and thickness. This dependence can also be experimentally proved, by plotting the values of grammage assessed for each patch as a function of the nanomat thickness (**Figure 13**). In the graph are shown the experimental data in terms of the percentage fiber volume $V_{f\%}$ (evaluated via Equation (13)) and are also reported the angular coefficient α of the linear regression lines for each type of membrane. Interestingly, as the nanofibers diameter increases (from Ny150 to Ny400) the slope of the linear regression line, and thus the angular coefficient α, increases ($G = \alpha\,t$). Consequently, it is worth pointing out that to obtain the same grammage with smaller nanofibers diameter (smaller α), it is necessary to electrospin thicker membranes.

This means also that smaller diameter nanofibers generate a higher percentage of porosity during the electrospinning deposition process. Indeed, rearranging Equation (13), higher diameters (higher α) correspond to higher $V_{f\%}$:

$$V_{f\%} = \frac{G}{\rho_m\,t} = \frac{\alpha\,t}{\rho_m\,t} = \frac{\alpha}{\rho_m} \tag{14}$$

Observing the experimental data (reported in the inset of Figure 13), a linear relationship between the diameter of the nanofibers and the percentage of fiber volume $V_{f\%}$ was found. The grammage-thickness plot allows to renormalize previous tensile tests in which the load had been normalized as a function of the cross-section area. In fact, having the calibration lines (in the present study reported for different Nylon 66 mats), it is possible to determine the grammage of any type of nanofibrous mat knowing its thickness. Therefore, given the grammage, it is possible to apply Equation (3) to obtain more reliable stress-strain curves based on grammage normalization of load. To apply this method, it is mandatory to adopt the same thickness measuring

tool used for the previous cross-section area normalizations. In the SI7 (Supporting Information) is reported the step-by-step procedure block diagram to recover previous tensile tests with load normalized respect to the specimen section.

4. Conclusions

The high porosity, flexibility, and deformability of nanofibrous nonwovens make troublesome their tensile testing, severely affecting results reliability. In this work, an accurate, systematic, and critical study concerning tensile testing of nonwoven mats, using electrospun Nylon 66 nanofibrous membranes as a case study has been presented. Three randomly oriented nanofibrous mats with different diameter (Ny150, Ny250, and Ny400) were produced and then morphologically, mechanically, and thermally characterized. In this frame, the "classical" approach to load normalization by means of specimen cross-section area was compared to a mass-based normalization proposed by the Authors, as well as a normalization based on the mat grammage, overcoming the trouble of the nanomat thickness measurement. The mass-based normalization method allows to obtain reliable and repeatable results, similarly to what happens for bulk materials. Although the grammage-based normalization is less reliable respect to the mass-based one, the use of mat grammage proved to provide better results than the "classic" normalization approach based on the specimen cross-section area. Moreover, the grammage-based method allows to re-normalize already tested specimens whose load–displacement curves were previously normalized on the cross-section area, thus benefitting of improved reliability and comparability of old data. Indeed, a linear dependence between these two parameters was found, whose angular coefficient depends on the nanofiber morphology.

Nanofibrous mat characteristics, such as nanofibers diameter, grammage, and specimen geometry (width and gauge length) were deeply investigated and the mats mechanical performance were interpreted also considering the polymer properties (degree of crystallinity and glass transition temperature), as well as the number of potential nanofibers crossings as a function of the nanofiber diameter. The tensile properties are found mainly dependent on the nanofibers diameter, which in turn strongly impacts the number of nanofibers crossings. Below a threshold value, which lies between 150 and 250 nm, the overall mat mechanical behavior changes from ductile to brittle. At the same time, the elastic modulus has a significant boost, while the mat strength is not affected. In particular, for the Ny150 membrane a Young's modulus of 1071 MPa was found, about three times respect to the other mats under investigation (296 MPa for Ny250 and 355 MPa for Ny400, respectively). Moreover, the experimental stress-strain data were analyzed using a phenomenological data fitting model to better interpret the tensile mechanical properties. The experimental results demonstrate the higher reliability of the proposed mass-based load normalization, providing a simple, effective, and universally applicable method for obtaining tensile stress–strain curves characterized by high reproducibility.

Supporting Information

Supporting Information is available from the Wiley Online Library or from the author.

Acknowledgements

The authors acknowledge the project "TEAM SAVE- E91B18000460007" (PG/2018/632196) of framework POR FESR 2014-2020 funded by Regione Emilia Romagna with DGR 986/2018 for financial support.

Conflict of Interest

The authors declare no conflict of interest.

Data Availability Statement

Research data are not shared.

Keywords

electrospinning, grammage, mass-based normalization of loads, mechanical properties, nanofibers, stress–strain, thickness

Received: March 19, 2021
Revised: April 24, 2021
Published online:

[1] BS EN ISO 9092:2019 **2019**.
[2] J. Nawab, *Textile Engineering*, De Gruyter, Berlin **2016**.
[3] S. J. Russell, *Handbook of Nonwovens*, Elsevier, Amsterdam **2007**.
[4] D. Semnani, in *Electrospun Nanofibers* (Ed: M. Afshari), Elsevier, Amsterdam **2017**, p. 151.
[5] A. Baji, Y.-W. Mai, S.-C. Wong, *Mater. Sci. Eng. A* **2011**, *528*, 6565.
[6] X. Qin, S. Subianto, in *Electrospun Nanofibers* (Ed: M. Afshari), Elsevier, Amsterdam **2017**, pp. 449–466.
[7] D. Lv, M. Zhu, Z. Jiang, S. Jiang, Q. Zhang, R. Xiong, C. Huang, *Macromol. Mater. Eng.* **2018**, *303*, 1800336.
[8] Q. P. Pham, U. Sharma, A. G. Mikos, *Tissue Eng.* **2006**, *12*, 1197.
[9] J. Ye, J. Si, Z. Cui, Q. Wang, K. Peng, W. Chen, X. Peng, S. C. Chen, *Macromol. Mater. Eng.* **2017**, *302*, 1700277.
[10] T. M. Brugo, E. Maccaferri, D. Cocchi, L. Mazzocchetti, L. Giorgini, D. Fabiani, A. Zucchelli, *Composites, Part B* **2021**, *212*, 108673.
[11] N. S. Abdel Rahman, Y. E. Greish, S. T. Mahmoud, N. N. Qamhieh, H. F. El-Maghraby, D. Zeze, *Carbohydr. Polym.* **2021**, *258*, 117643.
[12] D. Bonincontro, F. Fraschetti, C. Squarzoni, L. Mazzocchetti, E. Maccaferri, L. Giorgini, A. Zucchelli, C. Gualandi, M. L. Focarete, S. Albonetti, *Processes* **2020**, *8*, 45.
[13] H. H. El-Maghrabi, A. A. Nada, M. F. Bekheet, S. Roualdes, W. Riedel, I. Iatsunskyi, E. Coy, A. Gurlo, M. Bechelany, *J. Colloid Interface Sci.* **2021**, *587*, 457.
[14] P. Akangah, S. Lingaiah, K. Shivakumar, *Compos. Struct.* **2010**, *92*, 1432.
[15] D. Quan, F. Bologna, G. Scarselli, A. Ivankovic, N. Murphy, *Compos. Sci. Technol.* **2020**, *191*, 108065.
[16] E. Maccaferri, L. Mazzocchetti, T. Benelli, T. M. Brugo, A. Zucchelli, L. Giorgini, *Mater. Des.* **2020**, *195*, 109049.
[17] R. E. Neisiany, S. N. Khorasani, M. Naeimirad, J. K. Y. Lee, S. Ramakrishna, *Macromol. Mater. Eng.* **2017**, *302*, 1600551.
[18] D. Cocchi, F. Musiari, T. M. Brugo, A. Pirondi, A. Zucchelli, F. Campanini, E. Leoni, L. Mazzocchetti, *J. Adhes.* **2020**, *96*, 384.
[19] S. Merighi, L. Mazzocchetti, T. Benelli, E. Maccaferri, A. Zucchelli, A. D'Amore, L. Giorgini, *Polym. Eng. Sci.* **2019**, 59, 2541.
[20] E. Maccaferri, L. Mazzocchetti, T. Benelli, A. Zucchelli, L. Giorgini, *Composites, Part B* **2019**, *166*, 120.

[21] J. H. Wendorff, S. Agarwal, A. Greiner, *Electrospinning: Materials, Processing, and Applications*, Wiley, New York **2012**.
[22] BS EN ISO 10319:1996 **1996**.
[23] BS EN ISO 1924-2:2008 **2008**.
[24] BS ISO 1924-3:2005 **2005**.
[25] BS EN ISO 9073-2:1997 **1997**.
[26] BS EN ISO 534:2011 **2011**.
[27] X. Yu, C. Li, H. Tian, L.i Yuan, A. Xiang, J. Li, C. Wang, A. V. Rajulu, *Chem. Eng. J.* **2020**, *396*, 125373.
[28] X. Yang, Y.i Pu, Y. Zhang, X. Liu, J. Li, D. Yuan, X. Ning, *J. Hazard. Mater.* **2020**, *391*, 122254.
[29] F. Tuğcu-Demiröz, S. Saar, S. Tort, F. Acartürk, *Drug Dev. Ind. Pharm.* **2020**, *46*, 1015.
[30] S. Tiwari, A. Gaur, C. Kumar, P. Maiti, *Energy Fuels* **2020**, *4*, 2469.
[31] M. Mushtaq, M. Wasim, M. Naeem, M. Khan, S. Yue, H. Saba, T. Hussain, M. Siddiqui, A. Farooq, Q. Wei, *Coatings* **2020**, *10*, 484.
[32] A. Góra, L. Tian, S. Ramakrishna, S. Mukherjee, *Nanomaterials* **2020**, *10*, 1127.
[33] H. Gallah, F. Mighri, A. Ajji, J. Bandyopadhyay, *Polym. Adv. Technol.* **2020**, *31*, 1612.
[34] D. Chuan, R. Fan, Y. Wang, Y. Ren, C. Wang, Y. Du, L. Zhou, J. Yu, Y. Gu, H. Chen, G. Guo, *Compos. Sci. Technol.* **2020**, *192*, 108107.
[35] S. An, H. S. Jo, G. Li, E. Samuel, S. S. Yoon, A. L. Yarin, *Adv. Funct. Mater.* **2020**, *30*, 2001150.
[36] S. Hu, J. Wu, Z. Cui, J. Si, Q. Wang, X. Peng, *J. Appl. Polym. Sci.* **2020**, *137*, 49077.
[37] U. Y. Karatepe, T. Ozdemir, *Bioact. Mater.* **2020**, *5*, 510.
[38] S. J. Kim, B. M. Hong, W. H. Park, *Cellulose* **2020**, *27*, 5771.
[39] B. Li, F. Xiong, B. Yao, Q. Du, J. Cao, J. Qu, W. Feng, H. Yuan, *RSC Adv.* **2020**, *10*, 18614.
[40] E. Maccaferri, L. Mazzocchetti, T. Benelli, T. M. Brugo, A. Zucchelli, L. Giorgini, *Mater. Des.* **2020**, *186*, 108210.
[41] M. Gazzano, C. Gualandi, A. Zucchelli, T. Sui, A. M. Korsunsky, C. Reinhard, M. L. Focarete, *Polymer* **2015**, *63*, 154.
[42] O. Kallmes, H. Corte, *Tappi J.* **1960**, *43*, 73.
[43] R. E. Miles, *Proc. Natl. Acad. Sci. USA* **1964**, *52*, 901.
[44] S. J. Eichhorn, W. W. Sampson, *J. R. Soc., Interface* **2010**, *7*, 641.
[45] P. Chavoshnejad, M. J. Razavi, *Sci. Rep.* **2020**, *10*, 7709.
[46] C. J. Buchko, L. C. Chen, Y.u Shen, D. C. Martin, *Polymer* **1999**, *40*, 7397.
[47] K. Molnar, L. M. Vas, T. Czigany, *Composites, Part B* **2012**, *43*, 15.
[48] X. Zhang, X. Yang, G. G. Chase, *Sep. Purif. Technol.* **2017**, *186*, 96.
[49] T. Tanimoto, *Compos. Sci. Technol.* **2007**, *67*, 213.
[50] W. Li, Y. Zong, Q. Liu, Y. Sun, Z. Li, H. Wang, Z. Li, *Prog. Org. Coat.* **2020**, *147*, 105776.

